

# Flexible Bistable MEMS Bridges

J. Beharic<sup>\*</sup>, T.M. Lucas<sup>\*</sup>, Y.M. Senousy<sup>\*</sup>, C. K. Harnett<sup>\*</sup>

<sup>\*</sup> Electrical and Computer Engineering Department  
University of Louisville, Louisville, KY, 40217

## ABSTRACT

This paper describes the transfer of large-deflection MEMS devices from silicon and glass wafers to flexible and stretchy substrates, and explores their mechanical properties. Silicon dioxide ( $\text{SiO}_2$ ) ribbons and bridges have been transferred onto a stretchable substrate. Such structures can accommodate the high level of compressive and tensile strain needed for biomedical applications that require curvature sensing. An adhesion-based stamp technique to transfer the structures from a silicon wafer onto a flexible poly-dimethylsiloxane (PDMS) substrate has been developed. This dry-transfer technique replaces the wet etch technique and will open a new route to applications in switching and remote sensing with a low development cost.

**Keywords:** MEMS, flexible substrates, bistable, cantilever

## 1 INTRODUCTION

Modern techniques used in microelectromechanical systems (MEMS) sensor fabrication are adequate for use in most of today's planar devices, which do not require flexibility to function. However, it is difficult for a rigid structure to conform to curves and continually changing shapes that are commonplace in nature and biological applications [1]. Shape-aware deformable surfaces will transform everyday textiles into input devices. When applied to other objects, these membranes could continuously monitor subtle changes in the shape of skin, organs, and other natural or manufactured objects, including those with hidden geometry. In this work, we focus on the design, placement, and operation of ultra-low power compressed beams on flexible structures. A concept drawing can be seen in Figure 1. Unlike a strain gauge, these devices do not require amplification and do not require power to maintain their position. Therefore, power-consuming analog amplifier circuits and thick, heavy batteries could become unnecessary. This may lead to thin, lightweight sensors that do not alter the natural shape of a membrane.

This article discusses a set of oxide and metal bridges that have been transferred to a flexible poly(dimethylsiloxane) (PDMS) surface using dry-etch techniques. The transfer of large-deflection MEMS devices from silicon and glass wafers to flexible and stretchy

substrates was also performed to explore their mechanical properties. Due to the difference in thermal expansion coefficients between the  $\text{SiO}_2$  and PDMS, stress can be introduced into the bridges that causes them to deform to one of two stable states. Structures either buckle up or down with respect to the plane of the substrate. The mechanical relation of the stable and unstable states can be seen in Figure 2. By controlling the excess strain, the angle at which the bridges change state can be controlled, therefore allowing precise adjustment of the device's sensitivity.

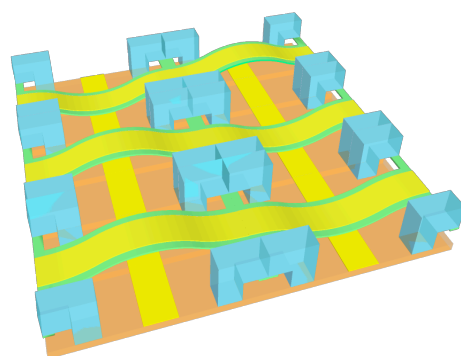


Figure 1: A 1-mm square patch with 6 MEMS bend-stretch sensors.

The beams have two stable states, "up" or "down." Switching behavior depends on the angle of the beam at the ends, as shown in Figure 2. This boundary angle is a function of the overall beam length, compression, and the substrate's radius of curvature. This implies that switches with different curvature thresholds can be created by changing either the amount of compression or the length of the suspended beam.

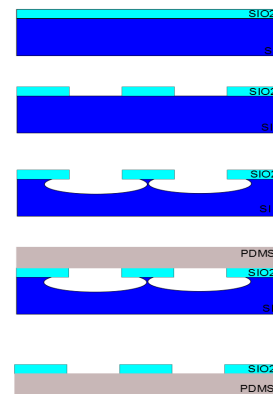
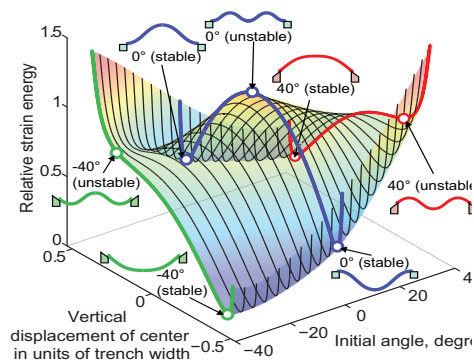


Figure 2: Energy landscape of bistable compressed beams as a function of surface angle at the ends.

Figure 3: Fabrication Diagram

An ohmic or capacitive readout of the "up" or "down" state would consist of two discrete values. Such a digital readout is simpler and lower in power consumption than analog sensing, and could enable batteryless operation powered by a radiofrequency (RF) reader.

## 2.2 Cleanroom Process for SiO<sub>2</sub>/Metal Bilayer Beams

## 2 FABRICATION

### 2.1 Cleanroom Process for Oxide Beams

The fabrication process of the devices is shown in Figure 3. The sequence begins with an oxidized silicon wafer of oxide thickness of 500 nm. Shipley 1813 photoresist is then spin-coated to the wafer and soft baked for two minutes at 115 C. The SiO<sub>2</sub> ribbons are patterned. After the wafer is exposed, the resist is developed in MF319 and hard baked for five minutes. The oxide ribbons are created using a Reactive Ion Etching (RIE) with specific parameters of: 12 minutes at 50% CF<sub>4</sub>, 3% H<sub>2</sub>, 260 mTorr, and 260W. The devices are then placed in a XeF<sub>2</sub> etch with the conditions of 20 cycles at 3 Torr XeF<sub>2</sub>, 0 N<sub>2</sub>, and 30 seconds; the devices are now ready to be bonded to PDMS. PDMS is mixed with a 10:1 hardener ratio, and once the PDMS has cured a small section is cut out and bonded to the SiO<sub>2</sub> ribbons on the wafer. In order to achieve bonding, the PDMS is cleaned with methanol and placed in air plasma to activate the surface for bonding. The PDMS and the ribbons on the wafers are pressed together and placed in an oven at 90C. After the two devices have been bonded, they are ripped apart leaving the oxide attached to the PDMS. An additional step of molding the PDMS is used to create oxide bridges, and a SU8 mold is created on a wafer. PDMS is then poured over the mold to create pillars, and the PDMS is then bonded to the device. Just as in the previous step, the PDMS is separated from the device leaving oxide suspended between two pillars.

To create these structures from metal, a similar processes is implemented. An additional two steps are required in the beginning of the process. First a 10nm/90 nm titanium/platinum (Ti/Pt) layer is deposited by sputtering. Once the metal has been deposited an intermediate layer of SiO<sub>2</sub> is deposited on the Pt using PEVCD. This additional layer will act as a bonding agent between the PDMS and the platinum. Once these additional steps have been completed the fabrication process follows the steps described in section 2.1.

## 3 FABRICATED DEVICES

The fabricated devices can be seen in Figure 3. The devices have a very uniform distribution. The image in Figure 4 shows the uniform distribution of the SiO<sub>2</sub> beams.

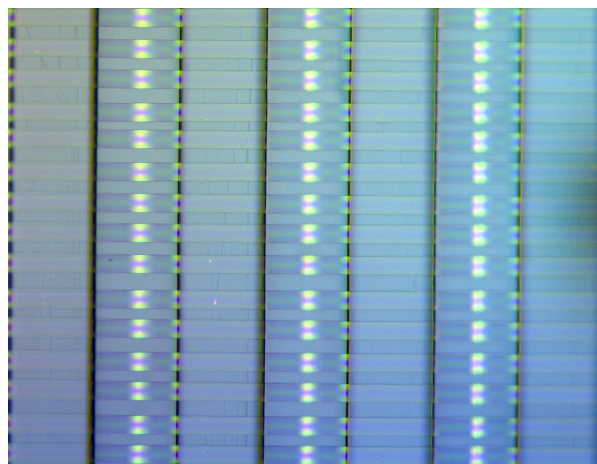


Figure 4: Optical image of SiO<sub>2</sub> beams

In addition to having a uniform distribution the devices also show uniformity in their buckling height. Optical surface profiler (Zygo) measurements show that the beams have a uniform 10  $\mu\text{m}$  height across all the beams. The profiler measurements of a single beam can be seen in Figure 5.

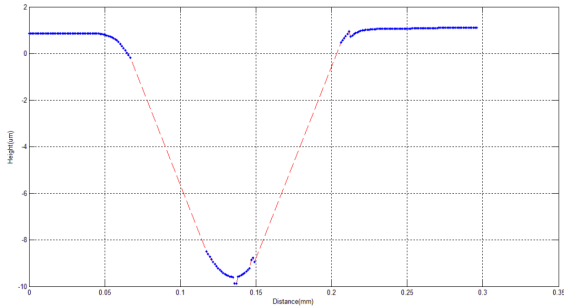


Figure 5: Zygo measurements

### 3.1 Preparing the samples for testing

In order to create functional devices, the beams must be placed at the material's "neutral plane" (halfway through the sample thickness for a uniform sample) to prevent the beam from just simply stretching. To accomplish this, a second piece of PDMS is bonded to another piece of PDMS onto which the beams have already been transferred. The second piece is then bonded perpendicular to the first piece. The resulting structure can be seen in Figure 6. Although bonding the second piece perpendicular to the first causes several of the beams to be unusable it allows large numbers of intact beams to be suspended at the neutral plane using a no-alignment process. Having a no-alignment process is important for scaling up to large area devices using an automated transfer method like roll-to-roll lamination.

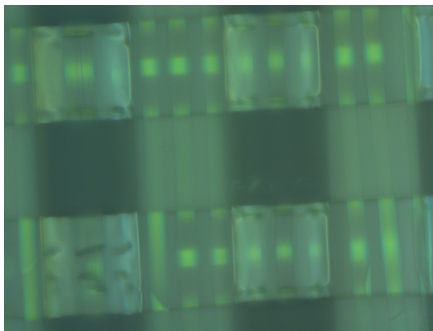


Figure 6: Image of two PDMS pieces bonded with intact bridges in the middle

### 3.2 Beam state detection

To determine the state of the bridges, a simple optical analysis was used. By applying side-lighting to the devices and optically observing the resulting image it is possible to

determine the state of beams. Figure 7. shows the setup which was used to determine the state of the bridges.

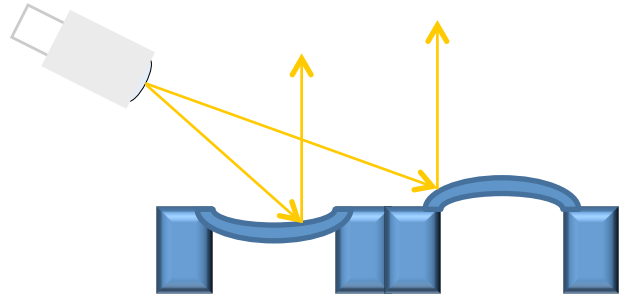


Figure 7: Side lighting technique for determining position of device.

The optical image clearly shows whether the bridges are up or down based on which side of the beam is illuminated. The resulting image of this setup can be seen in Figure 8. To further enhance and automate these reading image processing techniques can be used to evaluate the state of the beams over a large area

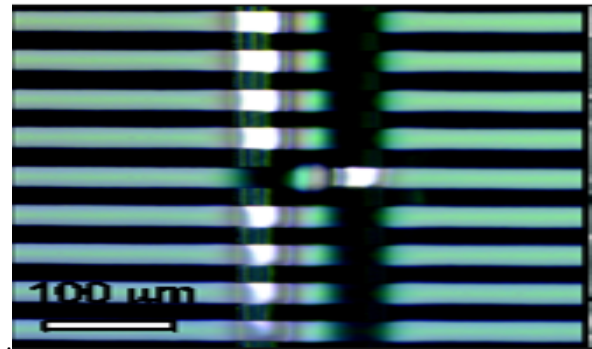


Figure 8: Optical Image of side-lighting Technique

## 4 RESULTS

The final product is bistable bridges that have been observed to maintain two different states, an "up" state and a "down" state. Figure 9 is a scanning electron micrograph of a single beam transferred to a PDMS substrate. In Figure 9(a) the beam is "up" and in Figure 9(b) it has flipped to "down." We attribute this to electron-beam induced charging of the suspended structure [3], causing electrostatic attraction between the beam and the PDMS substrate. Local thermal expansion due to electron-beam induced heating is another possibility; however, the beam in Figure 9 did not have a metal layer on it to perform differential thermal expansion. Uniform heating in an oven or on a hotplate causes the beams to stretch thanks to expansion of the PDMS[2]. However, the beams have built-

in hysteresis, and pure stretching does not cause them to cross the switching threshold. We have never observed these beams to change state using uniform heating from an oven or hotplate.

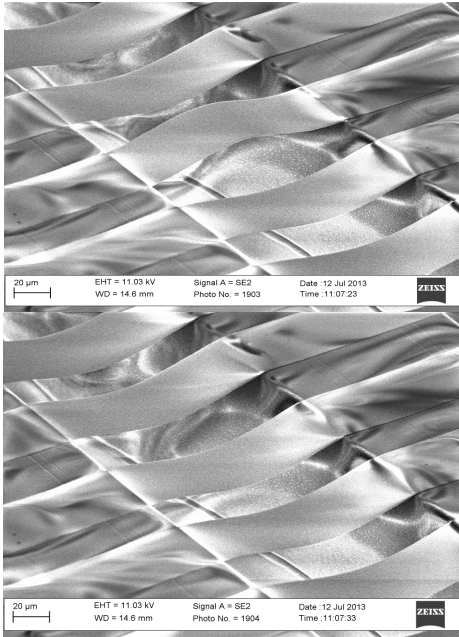


Figure 9: SEM image of a bridge switching between states (a) Image of bridge in “up” position (b) Image of bridge in “down” position

## 5 DISCUSSION

By adjusting the spacer length, these bridges can be tuned to a specific arch length that will trigger the devices to flip states at a set radius of curvature. In large macro-scale experiments the flipping behavior of a beam has been characterized using the geometric configuration shown in in Figure 10 [4]. The figure shows the relation of length  $w$  and the critical flipping angle  $\alpha$ . In this case, the length  $w$  is the spacing between the pillars. This can be used to extrapolate the compression ratio of  $\beta$ .

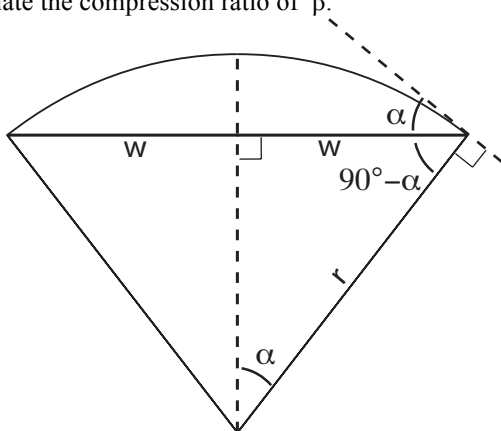


Figure 10: relationship between  $\alpha$ , the substrate curvature radius  $r$ , and the half-width  $w$

The compression ratio is modeled by the curve that is shown in Figure 11. The devices which have been featured in this paper have a compression ratio of 1.072, which corresponds to a critical angle of about 25 which is not possible to achieve with the devices discussed above. A more suitable critical angle can be achieved by increasing the length  $w$  and reducing the compression ratio with a lower bonding departure.

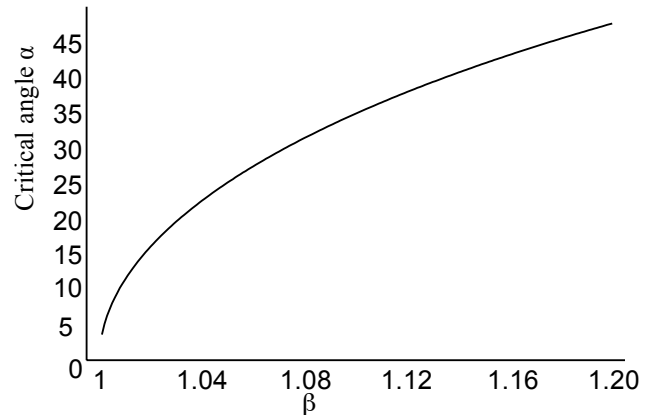


Figure 11: Critical angle vs compression ratio for three materials

## 6 CONCLUSION

We have successfully created suspended, compressed oxide microbridges on flexible, stretchable silicone substrates. These bridges can be made in large arrays, and can also be coated with metal either before or after fabrication, leading to electronic integration.

## ACKNOWLEDGEMENT

This work is supported by the Kentucky Science and Engineering Foundation as per Grant/Award Agreement # KSEF-2546-RDE-014.

## REFERENCES

- [1] D.-H. Kim, R. Ghaffari, N. Lu and J.A. Rogers, *Annual Review of Biomedical Engineering*, 14, 113-128 (2012)
- [2] D.Y. Khang, H. Jiang, Y. Huang and J.A. Rogers, *Science* 311, 208-212 (2006).
- [3] Satyalakshmi, K. M., Olkhovets, A., Metzler, M. G., Harnett, C. K., Tanenbaum, D. M., and Craighead, H. G., *J. Vac. Sci. Tech. B* 18, 3122-3125 (2000)
- [4] Beharic, J., Lucas, T. M., and Harnett, C. K., *J. Appl. Mech.* (in press) doi:10.1115/1.4027463 (2014)